(9)

ESO-74-D
July 1998

Fermilab Library
0 1160 0067555 7

Calibration of systematic optical path differences for the Very Large Telescope Interferometer (VLTI)

Samuel Lévêque, Bertrand Koehler
European Southern Observatory
Karl Schwarzschild str.2
D-85748 Garching bei München

SEP 17 1998

ABSTRACT

In stellar interferometery, the precise knowledge of systematic optical path differences is essential because it directly influences the ability to rapidly acquire fringes. Besides, when an object is too faint to provide a direct measurement of the fringe position error, the VLTI will provide the possibility to blindly track the fringes in open loop, according to the pre-calculated evolution of the OPD over time. In this case, a poor estimation of the OPD implies that the Delay Lines follow a trajectory, which progressively introduces residual OPD errors larger than the coherence length, and thus prevents further fringe observation.

The OPD model, which predicts the systematic OPD to be created by the Delay Lines is based on parameters representing the geometry of the interferometric array. When a direct measurement of these parameters cannot be easily implemented, such as in the VLTI, they can be determined by observing a set of calibration stars of known coordinates. This procedure, established as the Astrometric Calibration, traditionally takes into account only the Baseline vector and an internal OPD factor. Precise knowledge of the Baseline vector is also essential for the Narrow Angle Astrometric mode of the VLTI because any error on the Baseline vector directly influences the final astrometric accuracy.

In order to accurately determine the parameters included in the OPD Model by Astrometric Calibration, we propose an optimal selection of the calibration stars using a Genetic Algorithm. This selection method that we have validated by simulation, has also the advantage of minimizing the required number of calibration stars, thus reducing the time spent on calibration.

In interferometers using large telescopes, such as in the VLTI, sources of OPD errors correlated with the star position are potentially larger than in small-scale interferometers. We have identified the influence of the VLT unit telescope axis mis-alignments and modeled their effect on the optical path error. Furthermore, we have developed a simulation to explore the requirement to include the modeled axis mis-alignment parameters in an Astrometric Calibration according to the expected noise associated with the calibration process.

Keywords: optical long baseline interferometry, genetic algorithm

ESO-74-D

1. ASTROMETRIC CALIBRATION AND LIMITATIONS

Observing fringes with a stellar interferometer requires the continous displacement of delay lines as a result of diurnal motion. The equation traditionally used to compute as a function of time the systematic Optical Path Length to be created by the delay lines, noted DOPL, is given by:

$$DOPL = \vec{S}.\vec{B} + C$$

'$\vec{B}$' is the 3 dimensional Baseline vector of coordinates $[B_x, B_y, B_z]$. It is defined to a first order as the vector joining the intersection of the altitude and elevation axis of two telescopes of an interferometer. 'C' is the internal optical path difference, or delay constant, when the delay lines are at their reference positions and corresponds to an offset of the zero path difference position. Finally, $\vec{S}$ is the time dependent unit vector pointing towards the object under study whose elevation and azimuth angles are respectively noted E and A. According to the conventions adopted for the VLT, the star vector is given in the reference frame [West, South, Zenith] by:

$$\vec{S} = \begin{bmatrix} -\cos E.\sin A \\ \cos E.\cos A \\ \sin E \end{bmatrix}$$

By observing a set of N_c stars of known coordinates and by recording the optical path length (DOPL) necessary to observe fringes, a linear system can be formed which after inversion leads to an estimation of the parameters $[P]=[B_x, B_y, B_z, C]$ of the model[9]. The linear system, shown in Figure 1 is characterized by its Design Matrix, M. The estimated parameters can then be re-applied to estimate the OPD to be created by the delay lines to observe fringes from any science object.

On one hand, the accuracy on the estimated parameters is influenced by the noise $[\delta]$ occurring during the calibration process. This OPL noise is mainly introduced by the atmosphere: its standard deviation reaches about 25 µm (rms) in the expected environmental conditions on the VLTI site. $[\delta]$ cannot be significantly reduced even by increasing the observing time for each calibration star.

$$\underbrace{\begin{bmatrix} -\cos E_1 . \sin A_1 & \cos E_1 . \cos A_1 & \sin E_1 & -1 \\ \vdots & \vdots & \vdots & \vdots \\ \vdots & \vdots & \vdots & \vdots \\ -\cos E_{N_c} . \sin A_{N_c} & \cos E_{N_c} . \cos A_{N_c} & \sin E_{N_c} & -1 \end{bmatrix}}_{\substack{DesignMatrix: \\ M}} . \underbrace{\begin{bmatrix} Bx \\ By \\ Bz \\ C \end{bmatrix}}_{\substack{Parameters: \\ [P]}} = \underbrace{\begin{bmatrix} DOPL_1 \\ \vdots \\ \vdots \\ DOPL_{N_c} \end{bmatrix}}_{\substack{Measurements: \\ [DOPL]}} + \underbrace{\begin{bmatrix} \delta_1 \\ \vdots \\ \vdots \\ \delta_{N_c} \end{bmatrix}}_{\substack{Noise: \\ [\delta]}}$$

Figure 1: Linear system obtained for a 4 parameters model after observing N_c Calibration stars

On the other hand, the accuracy of the parameter estimation is strongly influenced by the conditioning characteristics of M which can only be improved by optimizing the selected calibration stars. For a given set of calibration stars, the Design Matrix may be ill-conditioned. For example, at elevation angles close to 90°, the third and fourth column of M become similar. Consequently, the effect of B_z and C are completely correlated and these parameters cannot be disentangled. In practise, the tendency towards ill-conditioning is accentuated by the limited coverage of the elevation angle of the telescopes. The elevation range is optimally 0°-90° but is further limited to 30°-90° while operating large telescopes such as the VLT to avoid mechanical deformations. The condition number of M, defined as $C_d=S_{max}/S_{min}$ (where S stands for singular value of M) characterizes how close M is from singularity . C_d represents an amplification factor on the impact of the noise $[\delta]$ as illustrated in Figure 2. The condition number entirely depends on the coordinates of the stars selected for calibration.

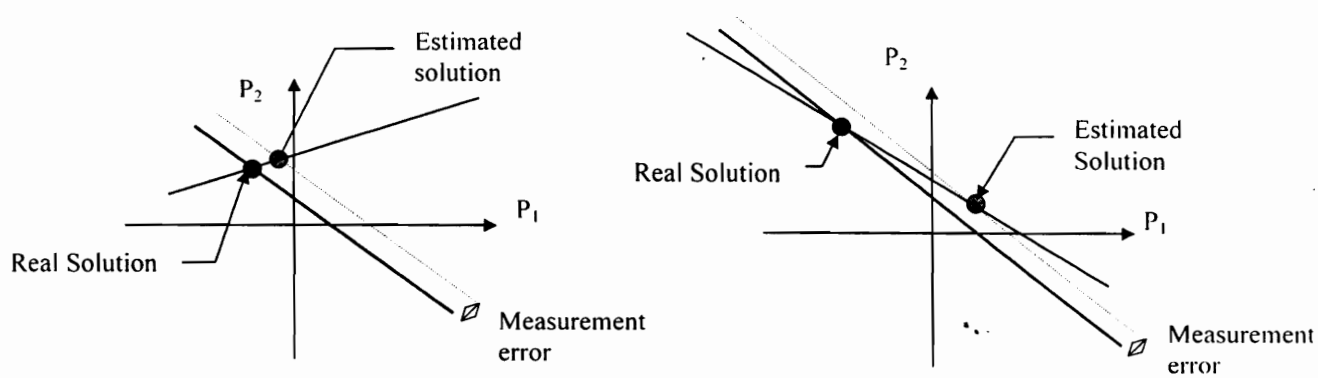

Figure 2: Graphical representation (in the parameter space) of the impact of C_d on the accuracy of the estimated parameters. Case of a two parameters problem P1 and P2. Left:Well conditioned system (small C_d); Right: poorly conditioned system (high C_d).

2. OPTIMUM SELECTION OF THE CALIBRATION STARS

We have investigated how to minimize the impact of the measurement noise associated with the Astrometric Calibration process by selecting a set of calibration stars which minimizes the Condition Number of the system's Design Matrix.

The difficulty of this problem is twofold. Firstly, it is not possible to analytically determine the coordinates of an optimum set of calibration stars because there is no analytical expression relating the Condition Number to the elevation and azimuth angles. Secondly, we are dealing with a large and discrete solution space because a possible set of stars must obviously corresponds to existing objects suitable for calibration. For example, selecting 10 different stars among 100 stars having a sufficient brightness, small angular extend, and appropriate spectral content, leads to $1.7\ 10^{13}$ solutions!

The implementation of traditional optimization techniques[8] would poorly perform. Indeed, in these techniques, the best solution is searched by using random guesses or gradient approaches. These methods also have the disadvantage of possibly getting trapped in local minima, to require continuous parameters for gradient calculation and are often limited to an optimization with few parameters.

Consequently, we propose to determine the optimum set of calibration stars by implementing a Genetic Algorithm (GA). Genetic algorithms are part of recent tools developed for optimization techniques where the natural processes of evolution and of genetic recombination are modeled[5,3]. GA's are able to operate on discrete parameters, to optimize problems having a large solution space where random searches would fail. This method is used in a continuously growing range of applications such as in machine learning[3] , in Fuzzy control systems[2] or in optimization of antennas[4]. A chronological list of applications is given in reference[3]. This is, to our knowledge, the first time that a genetic algorithm is applied to astronomical observations.

We first generated a catalogue (called *Iphcat)* from the FK5 catalogue, containing the coordinates of stars suited for astrometric calibration. We represented each star by a "gene" defined as the binary representation of the index of the star in *Iphcat*. A set of stars was represented by a "chromosome" obtained by concatenation of the genes associated with the stars (Figure 3). Therefore, a design matrix, *M*, could be associated to any chromosome. We defined the "fitness" of a given chromosome by the condition number of its associated Design Matrix. The fittest chromosome could be found by an iterative process and after decoding it provided the set of calibration stars for which the Design Matrix had a minimum condition number, i.e. lead to a well-conditioned system.

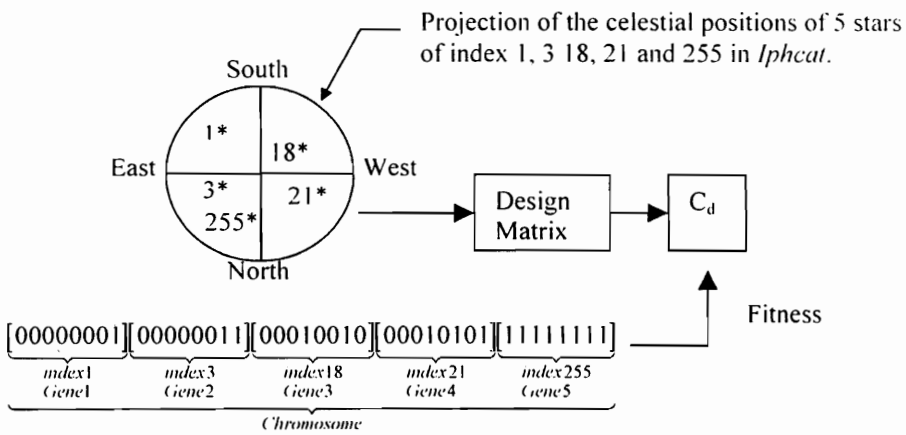

Figure 3: Chromosome representing a selection of 5 stars of index 1, 3, 18, 21 and 255 in the catalogue *Iphcat*

More precisely, the optimum solution was determined by first randomly selecting an initial population of chromosomes. All the chromosomes forming the initial population were then sorted in ascending order according to their fitness. Only the lower half chromosomes were selected for mating and cross-over, the upper half being rejected. The mating and cross-over of 2 parent chromosomes defined a pair of offsprings as illustrated in Figure 4. The cross-over position was randomly selected along the chromosome binary sequence. After paring all selected chromosomes, the creation of offsprings allowed to build a new population of chromosomes in which mutation could occur with a probability P_m. Mutation is the change of a small percentage of bits randomly chosen in the list of chromosomes. This operation allows the algorithm to search outside the current region of parameter space and avoid to get stuck in local maxima. Mutation was the last operation before to finally obtain a new generation. Then the fitness of each chromosome of this new population was evaluated. It was first necessary to decode each chromosome to retrieve the coordinates of the corresponding calibration stars and the corresponding condition number. In the nominal case, the algorithm led to a better solution for each generation.

The procedure was repeated during few hundred generations until a satisfactory solution appeared, that is when a better solution was not found after few tens of generations. The convergence time (the number of generations necessary to reach this solution) depends on the parameter space (how many stars do we need to find), on the solution space (how many different stars do we have in the catalogue), on the initial population number and on the probability of mating. Typically, the converging time was a couple of hours for an optimum selection of 20 stars, by running Matlab on a desktop computer. However, we were not constrained by the converging time.

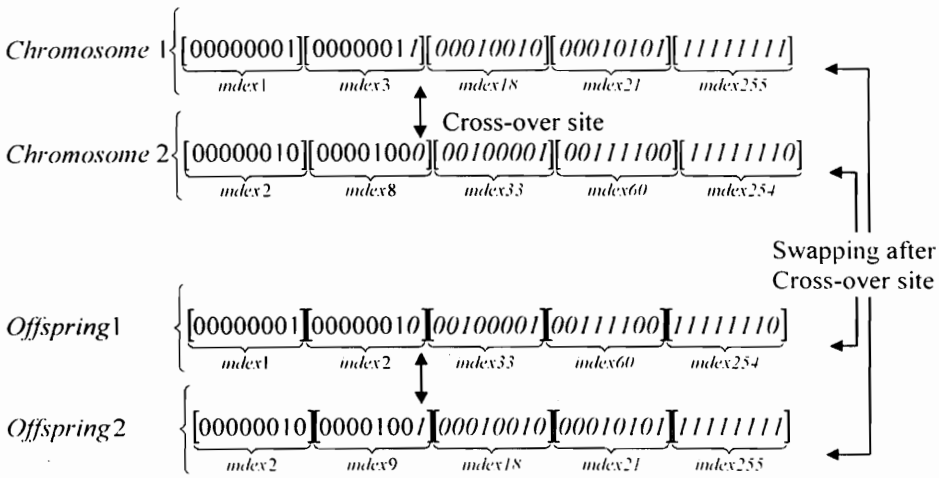

Figure 4: Mating and cross-over operations

3. VALIDATION OF THE SELECTION METHOD

3.1 Optimization of the condition number

In order to validate our selection method, we compared the condition number obtained for different star selection criteria:

- Random selection (S_R stars)
- Homogeneous distribution in the sky (S_H stars)
- Selection by our Genetic Algorithm (S_G stars)

An example is shown in Figure 5. This figure shows the distribution of 3 set of 8 stars selected according to the selection criteria listed above. We generated a homogeneous distribution of stars by tracing a spiral on the celestial sphere and by selecting the appropriate number of stars the closest to this spiral.

Figure 6 shows the effect of the star selection methods on the Condition Numbers of their corresponding design matrices. The form of the Design Matrix was given in Figure 1. Its ill-conditioning characteristic was already pointed out in section 1 for Elevation angles close to 90°. This explains why the 8 S_G stars partially avoid this region to better disentangle the B_Z and the C parameters during the later inversion of the linear system.

This phenomenon can be more precisely illustrated by computing the correlation between the parameters $[B_X\ B_Y\ B_Z\ C]$ calculated from the Design Matrixes obtained with the S_G and S_H stars. The correlations are given in Table 1 for both types of calibration stars. Since these Matrixes are symmetrical, we have only reported the lower triangular part. The results show that the S_G stars allow to efficiently reduce the correlation between the parameters and thus better disentangle them.

For a given Design Matrix M, we determined the correlations by first computing the Covariance Matrix[1], V, given by $V=(A^T.A)^{-1}$. The inversion was performed using a Singular Value Decomposition[8]. The diagonal elements of V, noted V_i,

i=1..4, are the variances of B_X, B_Y, B_Z, and C. The Correlation Matrix is given by R= D.V.D where D is a diagonal matrix whose elements D_i equal $(V_i)^{-1/2}$.

S_H	B_X	B_Y	B_Z	C
B_X	1			
B_Y	-0.37	1		
B_Z	0.83	-0.54	1	
C	0.84	-0.56	0.99	1

S_G	B_X	B_Y	B_Z	C
B_X	1			
B_Y	0.26	1		
B_Z	0.10	0.05	1	
C	0.13	0.18	0.95	1

Table 1: Correlation Matrixes for S_H and S_G stars

As expected, the results show that the Genetic Algorithm is a powerful way to select a set of data leading to a low Condition Number, that is a well conditioned system, even for a set of calibration stars containing a minimum of 4 stars. A gain of a factor 5 was obtained on the condition number compared to the results achieved with a homogeneous star distribution. The results obtained with the random star selection are only given for comparison as it highly depends on the draw of the random stars. The results confirm that a poorly selected set of calibration stars can have a significant impact on the system conditioning. This implies in particular that previous observation of scientific targets is not necessarily optimum to estimate the parameters of the OPD Model.

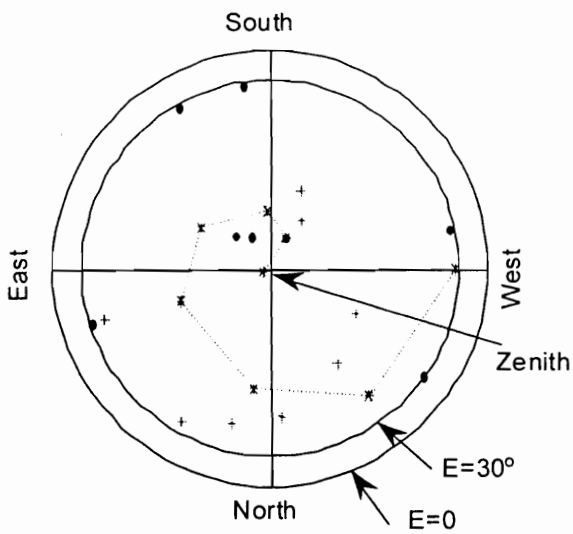

Figure 5: Projection of star position for 8 calibration stars
•: Selection using the genetic algorithm S_G; *: using an Homogeneous distribution, S_H; +: random distribution, S_R

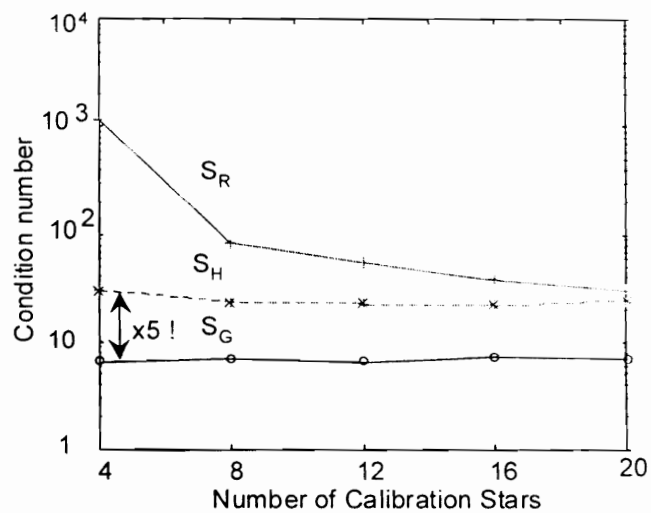

Figure 6: Condition number of the design matrix associated with the set of calibration stars (S_R, S_H, S_G).

3.2 Accuracy on the estimated parameters and Fringe acquisition error

The objective of this simulation was to compare the performance of the 3 types of selection methods on the determination of the Baseline Vector and on the Fringe Acquisition performance. We chose a given parameter vector [P]. In our simulation it corresponded to an operation with the VLT unit telescopes UT1 and UT2 and a delay constant, C, of 1m. For each set of stars S_R , S_H and S_G, we simulated both the calibration and the parameter fitting procedures to estimate 3 parameter vectors $[P_c]_{R,H,G}$. The Simulation Data flow is presented in Figure 7. The matrix $[M_{R,H,G}]$ represents the Design Matrices corresponding to each set of calibration stars.

We assessed the influence of the number of calibrator stars N_c by using a number of stars of type S_R , S_H and S_G ranging from 4 to 20. In order to have a representative calibration procedure, we added the same 25μm rms noise (normally

distributed) to all types of measurements. The estimations of the parameters were performed by inverting the Design Matrixes using Singular Value Decomposition (SVD) before to conclude on the respective performance of the 3 selection methods.

In a second step, we investigated how the error made on the parameter vector influenced the Fringe Acquisition performance for any object in the sky. The procedure is illustrated at the bottom of Figure 7. Hence, depending on the coordinates (E,A) of an object, we first computed the factor $DOPL_r$ necessary to observe this object using the real parameter vector [P]. Then for the same object, we computed the estimated $DOPL_e$ by using the estimated parameter vectors $[P_e]_{R,H,G}$. The quadratic error, noted $\varepsilon_{R,H,G}$, between $DOPL_r$ and $DOPL_e$ computed for any object, represented the Fringe Acquisition error induced by an estimation error of the parameter vector.

Calibration Procedure and Parameter Estimation

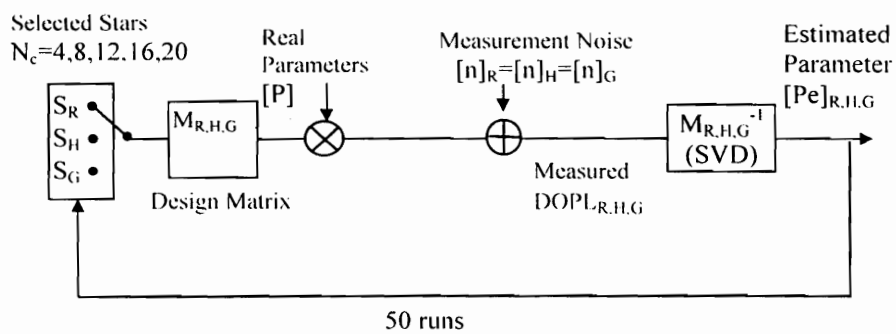

Performance on Fringe Acquisition

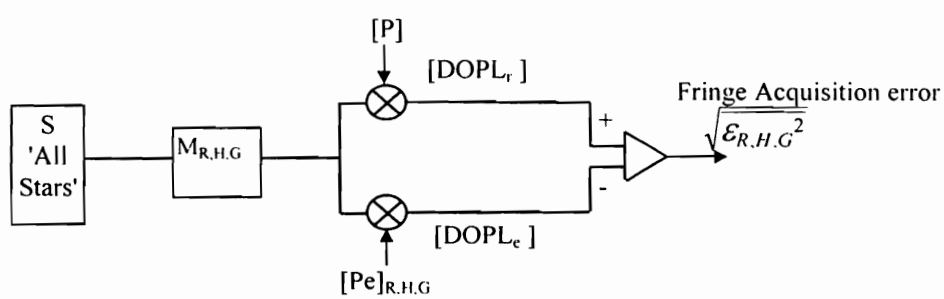

Figure 7: Simulation data flow

The results shown in Figure 8 demonstrate that it is possible to determine the Baseline vector with a 50 μm accuracy which corresponds to the demanding Narrow Angle Astrometry requirements of the VLTI[10]. A Baseline error of less than 50 μm can be already obtained for 8 S_G stars whereas an equivalent performance is only reached for at least 20 S_H stars. Therefore, by carefully choosing the calibration stars, a gain of a factor 2.5 can be achieved on their necessary number. Considering that a minimum time of 3 minutes is required to point the telescope and acquire fringes on an object during calibration, the results show that our method provides a time saving of about 60-24=36 min. Furthermore, the Baseline error can be reduced to the noise level with 20 S_G stars.

Results on the Fringe Acquisition performance are summarized in Figure 9. The mean fringe position error obtained with 4 S_G stars is only reached with 16 S_H stars which corresponds to a calibration time of respectively 12 min and 48 min.

The advantage of our method is that only a reduced number of calibration stars are necessary to perform an accurate Astrometric Calibration thus substantially reducing the impact of the time spent on calibration. This aspect is particularly relevant considering the time pressure set on the VLT Unit telescopes.

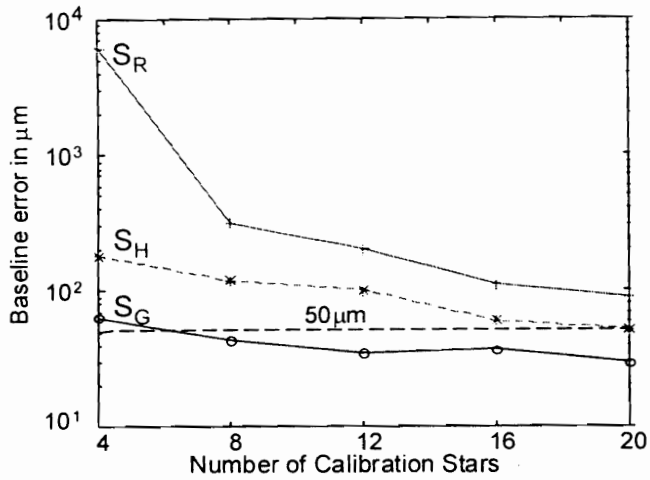

Figure 8: Error on the baseline obtained for 3 star selection criteria. • :genetic algorithm S_G; Homogeneous distribution, S_H; +: random distribution, S_R

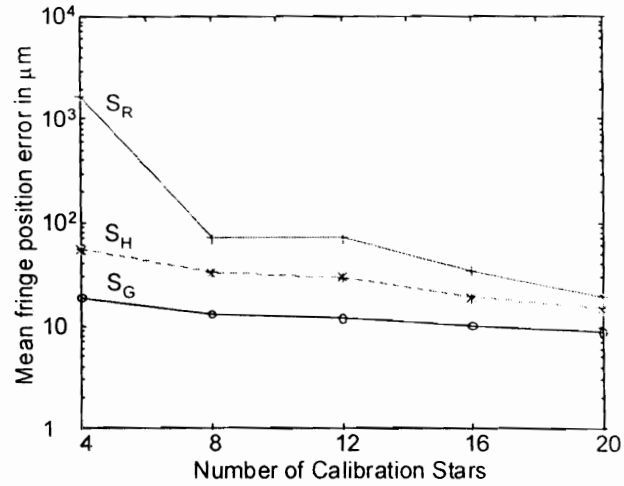

Figure 9: Mean fringe position error over all sky positions when the estimated parameters are re-applied to predict the fringe position.

4. INFLUENCE OF TELESCOPE AXIS MIS-ALIGNMENT ON SYSTEMATIC OPD ERRORS

The effect of mechanical imperfections of the telescopes on the Baseline vector or on the delay constant has already been reported in small scale interferometers operating with siderostats[7] . These OPD errors were attributed to axis misalignments, run-outs or ball-bearing errors. In the case of VLTI, the axis misalignment and run-outs of the Unit Telescopes are expected to reach few 100 µm and the monitoring of a mean pivot point cannot be practically implemented.

Using sensitivity matrices, we have modeled the effect of the main types of axis misalignments inside a telescope, which introduce OPD errors:

- Run-outs
- Bearings imperfections (swash=axial displacement along Elevation or Azimuth axis)
- Mean separation between the Azimuth and Elevation axis

The results show that the combination of some of the components of the Run-outs and swash first harmonic, mimic Baseline or Delay Constant errors. Therefore, these mis-alignments are already implicitly fitted during an Astrometric Calibration process similar to the one presented in Figure 1. The true additional effect of the axis misalignments on systematic OPL errors is given by the following 3 independent parameters:

Parameters	Origin	Basis Function
ΔTEC	Combination of Elevation run-outs and swash and of axis mean separation	cos(E)
ΔTSAS	Telescope swash in Azimuth (sine component)	sinA.(1-sinE)
ΔTSAC	Telescope swash in Azimuth (Cosine component)	cosA.(1-sinE)

Table 2

The impact of these 3 parameters on the OPL as a function of elevation and azimuth angles is shown in Figure 10. In the case of the VLTI, a maximum error of about 300 μm is expected to occur during Fringe Acquisition. This error should not significantly affect the Fringe Acquisition procedure because a minor scan of the delay lines would be required to observe fringes. During Blind mode observation, an OPD error equivalent to the expected 25μm rms noise (cf.section 1) would only be reached after 20 min of blind observation. This result is compatible with the mean blind observing time of about 10 min. Therefore, on average Blind observation should not be affected by Telescope axis-misalignment.

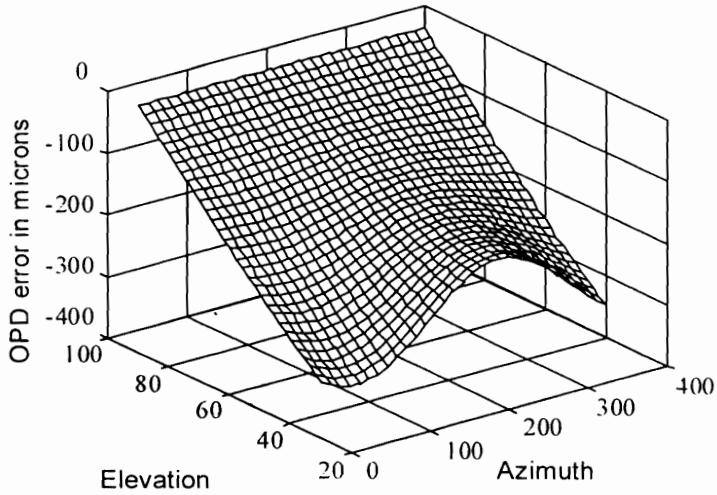

Figure 10: Independent OPD error due to telescope axis mis-alignment.

Although the direct impact of the mis-alignment parameters on the OPD error is relatively small, this does not ensure that an OPD Model using only the factors *[Bx By Bz C]* has a sufficient accuracy in presence of axis-misalignments. In this case, the estimation of these 'traditional' parameters could be impaired by modeling errors which act during the calibration process as a supplementary noise on the measurements [DOPL] (Figure 1). We have developed a simulation (similar to the one presented in Figure 7) to assess to what extend can modeling errors influence the accuracy of the Baseline vector and the Fringe Acquisition performance. The real parameter vector *[P]* included *[Bx By Bz C TEC TSAS TSAC]* whereas the fit was performed respectively on the estimated parameter vector $[P_e]$= [*Bx By Bz C*] and *[Pe]*= [*Bx By Bz C TEC TSAS TSAC*]. In both cases the calibration stars were selecting using the Genetic algorithm presented in section 2.

The results, presented in Figure 11 and 12, show that it is necessary to fit the axis-misalignment parameters to possibly reach the accuracy goal imposed by Narrow Angle Astrometry with the VLTI (50μm). The reason is that when confronting the 'traditional' model to the measurements (which are based on the 'real' model), these measurements includes OPD offsets which amount on average 140 μm (cf Figure 10) and are therefore significantly larger than the 25 μm rms noise level. In this case, the measurements contains outliers points which are sufficient to impair the robustness of the solution determined by the least square fit[1]. Including the mis-alignment parameters in the OPD Model has also the advantage of providing a Fringe Acquisition accuracy limited by atmospheric noise with a limited number of Calibration stars

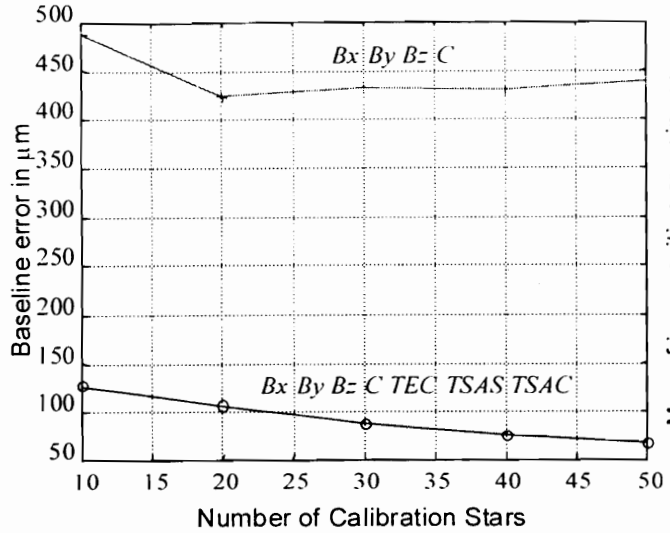

Figure 11: Baseline error in presence of axis-misalignment and depending on the parameters included during astrometric calibration

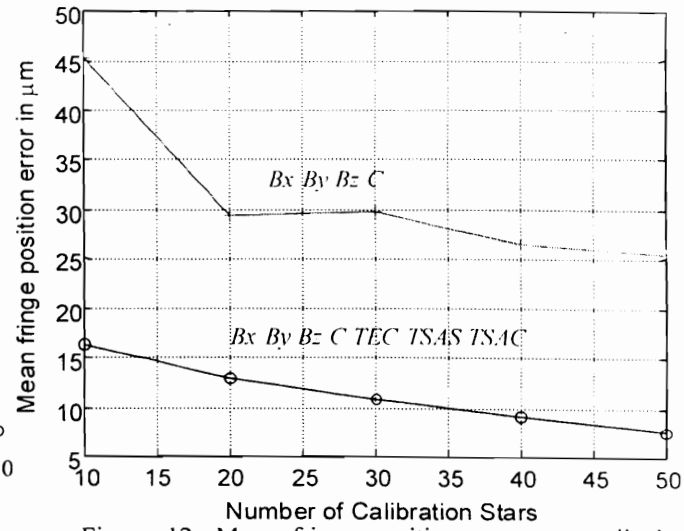

Figure 12: Mean fringe position error over all sky position depending on the parameters included during astrometric calibration

5. CONCLUSION

In order to accurately determine the parameters included in the OPD Model by Astrometric Calibration, we proposed an optimal selection of the calibration stars using a Genetic Algorithm. This selection method has the advantage of minimizing the required number of calibration stars, thus reducing the time spent on calibration. We have modeled the impact of the telescope axis misalignments on systematic OPD errors. The amplitude of these mis-alignments indicates that this impact is a-priori marginal on the Fringe Acquisition and Blind Tracking performance. However, we developed a simulation to more precisely assess the impact of modeling error, i.e. when the axis misalignments are not included in the OPD Model. The results show that it is indeed necessary to fit the axis-misalignment parameters to reach the accuracy goal imposed by Narrow Angle Astrometry upon the Baseline vector. Furthermore, including the mis-alignment parameters in the OPD Model has the advantage of providing a Fringe Acquisition accuracy limited by atmospheric noise with limited number of calibration stars.

6. REFERENCES

1. Branham R.L, "Scientific Data analysis, an introduction to over-determined systems", ISBN 0-387-97201-3, Springer Verlag, 1990.
2. Del Castillo Sobrino D. ,"Genetic processing of the sensorial information", Sensors and Actuators, 37-38, 25, 1993.
3. Goldberg D., "Genetic algorithms in search, optimization and machine learning", Addison-Wesley publishing company Inc., ISBN 0-201-15767-5, 1989
4. Haupt R., "An introduction to Genetic Algorithms for Electromagnetics", IEEE Antennas and propagation magazine, Vol.37, No.2, April 1995
5. Holland J., "Genetic Algorithm", Scientific American, July 1992, p.44
6. Lévêque S., "Methods and Laser systems for the analysis of the internal optical path for the VLTI", Ph.D. Thesis, ULP Strasbourg, 1997
7. Mozurkewich D. et al, "Preliminary measurements of stars positions with the Mark III stellar interferometer", AJ vol.95, n.5, 1988.
8. Press W.H. et al, "Numerical recipes in C", Cambridge University Press, ISBN 0-521-43108-5, 1995
9. von der Lühe O. , A.Quirrenbach , "Calibration of the VLT interferometer", ESO/ST-ECF workshop, Calibrating and understanding HST and ESO instruments, ESO Garching 25-28 April 1995.
10. von der Lühe O., A. Quirrenbach, B. Koehler, "Narrow-Angle Astrometry with the VLT Interferometer", Proceedings of the ESO Workshop Science with the VLT, 28 June-1July 1994, Springer Verlag 1995(b).